Modern Noninvasive Measuring Techniques for Transient Two-Phase Flow

F. MAYINGER
Technical University Munchen
Munchen, FRG

ABSTRACT

A noninvasive measuring technique must not influence the thermo- and fluid-dynamic behaviour of the flow or interfere with the physical phenomenon to be investigated. Sensors for fulfilling this condition are mainly waves of various characters.

Optical methods play an important role in noninvasive measuring techniques. Out of this family image forming and nonimage forming methods, like the holographic interferometry, the light scattering, and the Laser-Doppler methods are presented.

Non-optical methods use mainly γ-ray or X-ray attenuation. Also here we can distinguish between image forming and nonimage forming methods. Finally, the application of more rarely used methods, like Raman scattering and sound waves reflection, are discussed.

1. INTRODUCTION

"Noninvasive" means that the sensor of the measuring technique has no interaction with the fluid to be investigated and that the phenomena of interest and the physical behaviour are not affected at all. Strictly speaking, this is only the case if the sensor has dimensions which are only in the order of the size of molecules or of the mean free path-length between the molecules. These conditions can be only fulfilled by waves - optical, electromagnetic, ionizing ones or sound waves. For optical waves the fluid must be transparent and electromagnetic waves can only be used if the conductivity or the impedance of the fluid is high enough. Ionizing beams are widely used in two-phase flow measuring techniques, mainly γ- or X-rays because of their stronger penetration ability compared to α- or β-rays.

Looking from another point of view, we can subdivide these noninvasive techniques in such ones which use only the attenuation, the scattering or the deflection of the beam. In all these cases under investigation the fluid is influencing the "sensor" but not the "sensor" the fluid.

Within the given frame of this paper it is not possible to discuss all noninvasive techniques proposed for measurements in two-phase flow and, therefore, here only examples of noninvasive techniques will be selected which are more frequently used in two-phase flow.

2. OPTICAL METHODS

2.1 Image Forming Methods

Optical methods are using light in its visible range sometimes also in the infra-red spectrum. They are known for many years in heat and mass transfer and also in two-phase flow because of their unique advantages. Besides not influencing the process examined they allow inertialess measurements and they, therefore, can be used for investigating even ultra-fast phenomena. Instead of point-by-point measurements, informations about a whole field can be obtained by the evaluation of photographs, for example.

Optical methods are especially suitable if one wants to visualize the flow pattern or the phase distribution of a gas-liquid-flow. It is also possible to photograph the droplets in a spray- or fog-flow, however, in this case the holography as compared to photography has some advantages, as we will see later. To get clear and well-defind outlines of the copied droplet or phase boundary ultra short-time exposures have to be made.

Usually photographs are taken rectangular to the flow direction through a transparent wall made of glass, for example. With this special technique, however, disturbances and even falsifications have to be expected by the liquid film flowing along the wall. Therefore, Arnold and Hewitt /1/ proposed another method which takes photographs of the two-phase mixture coaxially to the flow. This method is the only one of the techniques known which allows also to make clearly outlined pictures of very highly transient processes. A sketch of the optical arrangement is shown in FIG.1a.

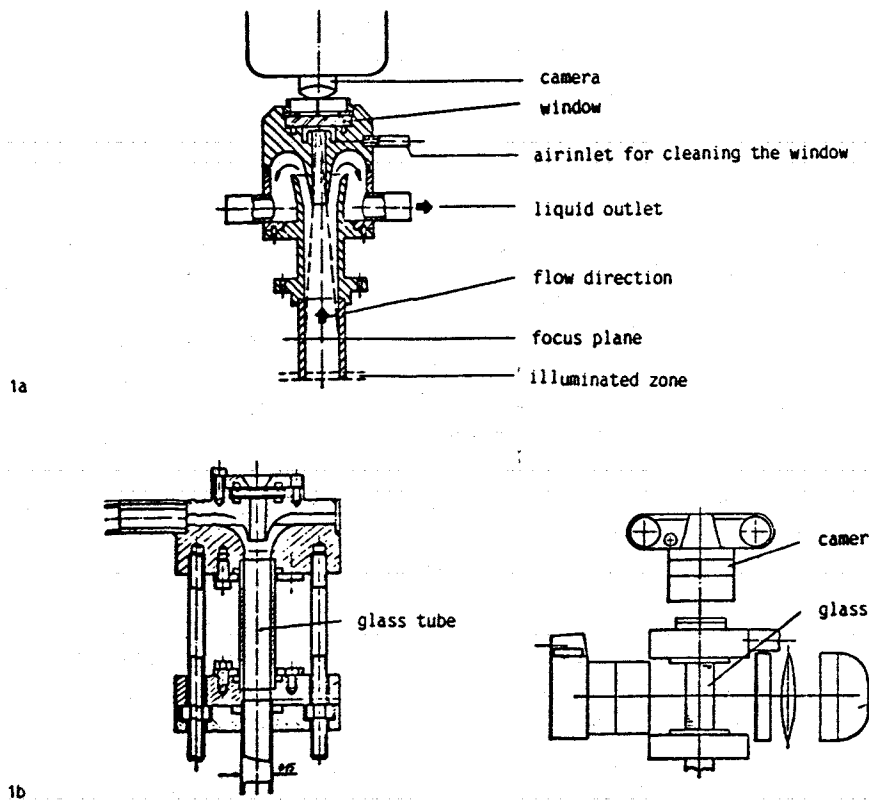

FIGURE 1. Optical arrangements for axial measurements in two-phase flow.

Langner /2/ altered this arrangement in some details, as shown in FIG.1b.

At the end of an electrically heated tube a flow splitter is placed which allows a separation of the liquid film at the wall and the gas core in the center entrained with droplets. At the top of the flow separator a lense is placed through which the flow can be observed, photographed or filmed in axial direction. The lense must be manufactured very precisely by using glass of high quality to avoid reflections. Following the heated test section a short glass tube is arranged through which the fluid can be illuminated from outside. The transition between heated steel tube and glass tube has to be smoothed very carefully to avoid disturbances of the flow.

The advantage of this special technique versus the usual methods photographing rectangular to the flow is demonstrated in FIG.2. The view from the top into the tube offers clear information about the radial droplet distribution and droplet form.

FIGURE 2. Photograph of flow pattern in two-phase flow.

As "registration apparatus" a usual camera or any high-speed movie-camera can be used. Both types of cameras, however, need a focussing screen in the form of a ground glass to control the range within the tube in which a visual observation is intended. Missing this ground screen, a very complicated calculation for metering the focussing distance would be needed, involving the exact knowledge of the geometrical-optical data of the camera and its lenses. Telelenses of long focussing distance show great advantages because they are forming an image with clear and well-defined outlines within only a very narrow range.

High-speed cinematography. The usual arrangements and methods of high-speed cinematography using a high-frequency flash or stroboscope and a film camera or a drum-camera are well known. These devices and methods are usually good up to exposure frequences of 10 to 20 kHz with exposure times of approximately 10^{-6}s. If shorter exposure times and shorter periods between two exposures are needed, a special arrangement called Cranz-Schardin-camera can be used, as shown in FIG.3. This device allows exposure times

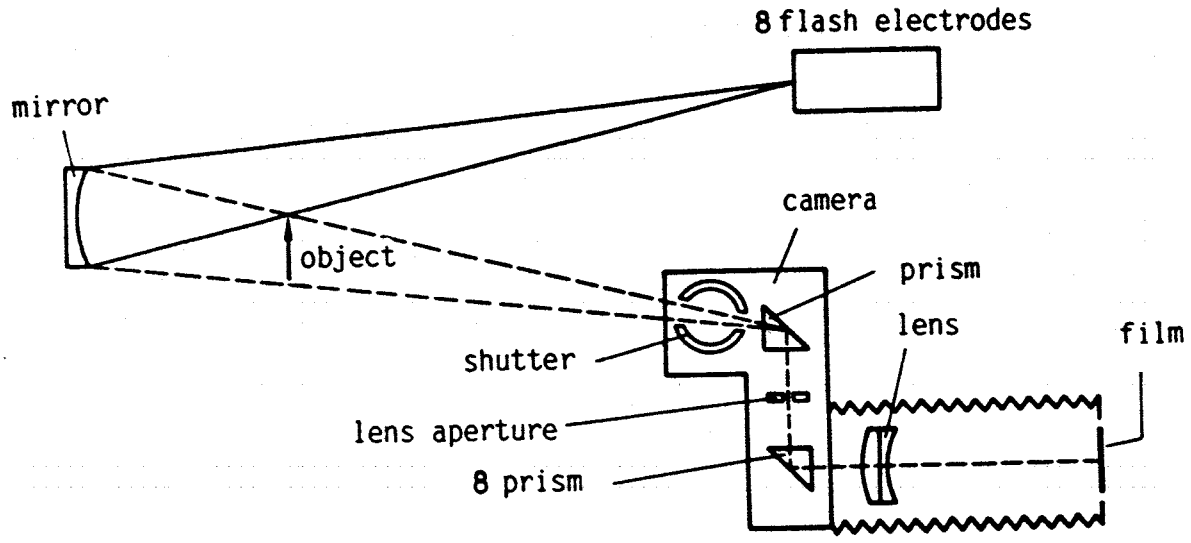

FIGURE 3. Cranz-Schardin-camera for ultra short-time cinematography.

down to 10^{-8}s with intervals between two exposures variable from several seconds to some micro-seconds. However, the number of pictures taken in one series is limited depending on the number of electrodes producing the flashes.

The electrodes are ignited in the desired intervals and each flash is producing an image via the parabolic or spheric mirror and a prism. The electrodes are arranged in one plane, however, displaced horizontally and vertically. Due to this arrangement also the pictures produced by the series of flashes are displaced and all pictures can be registered on one photographic plate. The shutter of this Cranz-Schardin-camera is open until all flashes are ignited. By this method it is possible to register even very tiny particles flowing with an extremely high velocity, as FIG.4 demonstrates. The photograph in FIG.4 shows two exposures taken in a time distance of 10^{-5}s of a small liquid membrane in the nozzle of a venturi-scrubber flowing with a velocity of 80 m/s. From the two exposures registered on one photographic plate not only the velocity and its direction but also the deformation of the membrane can be easily and exactly evaluated.

The optical methods discussed up to now allow to improve the comprehension of the phenomenology of gas-liquid-flow and also to evaluate the velocity and its direction. In many cases, however, the flow of gas-liquid- or vapour-liquid-mixtures is affected by the heat transfer. In these cases also the temperature distribution near the heated wall or near the phase interface are of interest. In single-phase flow optical interference methods for registering the temperature fields in fluids are in use since a long time, as for example the Mach-Zehnder-interferometer. All these methods, however, demand a so-called comparison-object in which all fluid-dynamic phenomena are identical with that in the test area, with the only exception that the comparison-object is not affected by heat transport. For vapour-liquid-mixtures such comparison conditions being exactly in

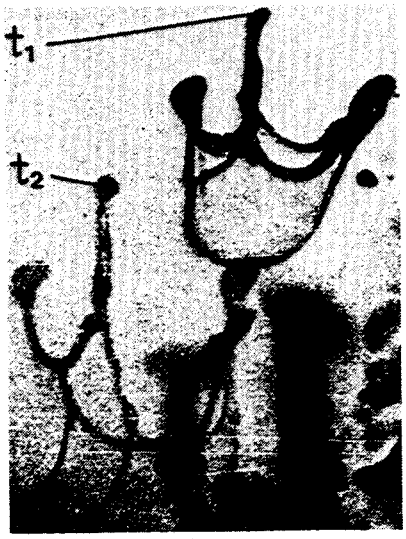

FIGURE 4. Double-exposure photograph of a liquid membrane in a Venturi-scrubber.

phase with the process in the tested area cannot be produced or verified. Therefore, another method - the so-called holographic interferometry - is used.

Holography and holographic interferometry. In 1949 Gabor /3/ invented a new optical recording technique which he called "holography". In contrast to photography, by which only the two-dimensional irradiance distribution of an object is recorded, holography allows the recording and reconstruction not only of the amplitude but also of the phase distribution of wave fronts. Making use of this unique property completely new interference methods could be developed. As holography demands a highly coherent light source, it can be only performed by using a laser.

The general theory of holography is so comprehensive that for a detailed description one must refer to the literature /4-6/. Here only the principles necessary for understanding the holographic measurement techniques can be mentioned. In FIG.5 the holographic two-step image-forming process of recording and reconstructing an arbitrary wave front is illustrated. The object is illuminated by a monochromatic light source and the reflected scattered light falls directly into a photographic plate. This object wave usually has a very complicated wave front. According to the principle of Huygens we can, however, regard it to be the superposition of many elementary spherical waves. In order to simplify the matter only one wave is drawn in FIG.5. This wave is superimposed by a second one, called "reference wave". If both waves are mutually coherent they will form a stable interference pattern when they meet on the photographic plate. This system of fringes can, therefore, be recorded on the photographic emulsion. After the development the plate is called "hologram". The amplitude is recorded in the form of different contrast of the fringes, and the phase in the spatial variations of the pattern.

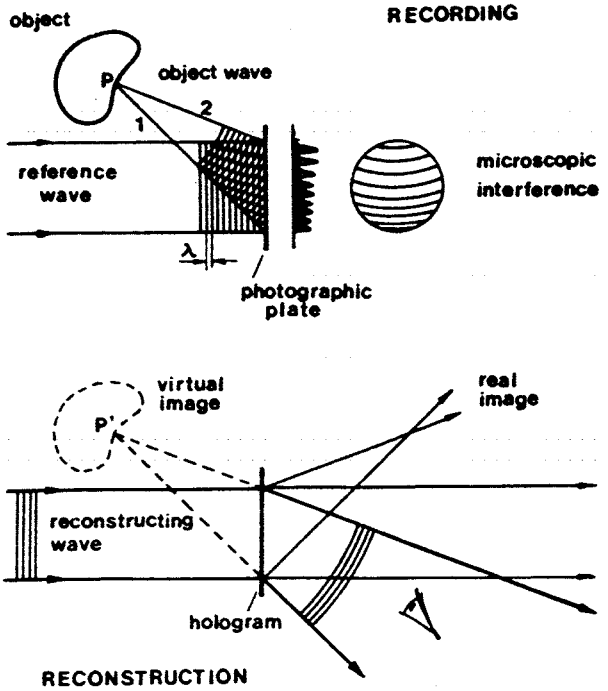

FIGURE 5. Holographic two-step image forming process.

If the plate is subsequently - after chemical processing and development - illuminated by a light beam similar to the original reference wave, the microscopic pattern acts like a diffraction grating with variable grating constant. The light transmitted consists of a zero-order wave travelling in the direction of the reconstructing beam plus two first-order waves. One of these first-order waves travels in the same direction as the original object wave and has the same amplitude and phase distribution. Thus a virtual image is obtained. The other wave creates a real image of the object.

This holographic technique can be used instead of the photography, for example for recording a swarm of droplets produced in a high-pressure injection-nozzle, as demonstrated in FIG.6. Because no lenses are used, no focussing plane exists; rather the whole volume of the droplet swarm can be reconstructed - with clear outlines of the droplets - from the hologram. FIG. 6a shows a reconstructed plane out of the droplet swarm and demonstrates that very tiny droplets or particles can be registered and observed.

Since in heat and mass transfer the temperature and concentration distribution in fluids is of special interest, a slightly different method is used, instead of that described in FIG.5. Instead of recording a reflected wave, the object wave having passed through the fluid in which the heat and mass transfer occurs is recorded.

A most commonly used arrangement of optical set-ups for holographic interferometry is shown in FIG.7. A helium-neon-laser or an argon-laser serves as a light source. By means of a beam splitter the laser beam is divided into an object- and a reference-beam. Both beams are then expanded to parallel waves by a telescope which consists of a microscope objective and a collimating lense. The object wave passes through the test section in which the temperature is to be examined, whereas the reference wave directly falls onto the photographic plate.

6a

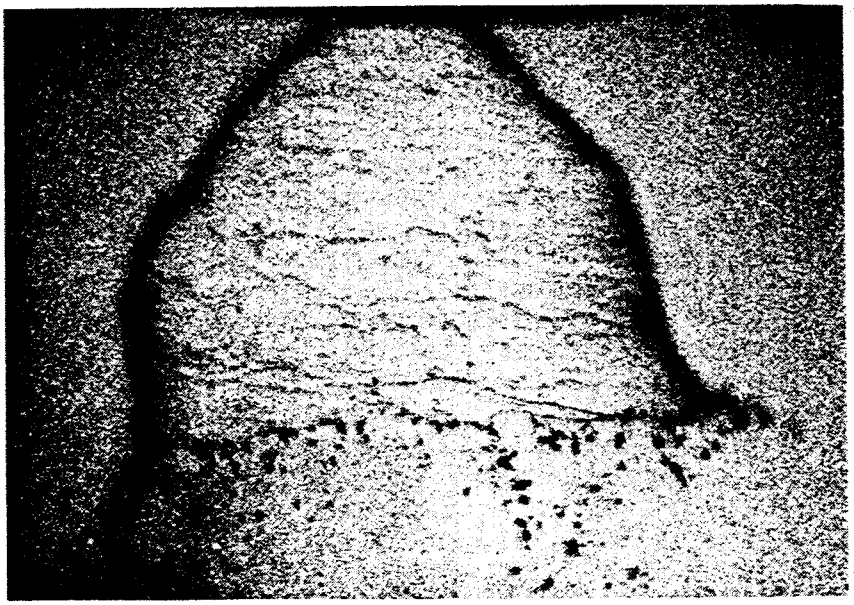

6b

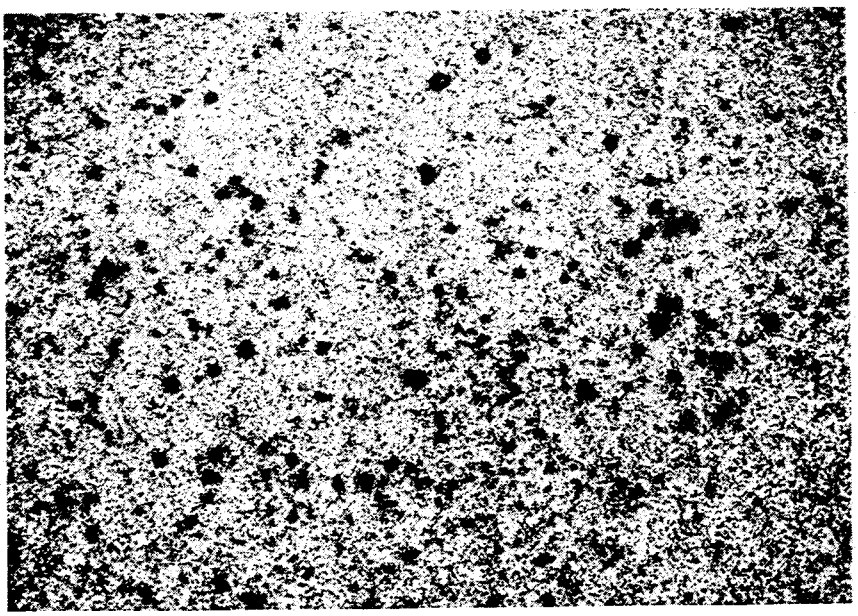

FIGURE 6. Holograms of droplet swarms after an injection-nozzle.

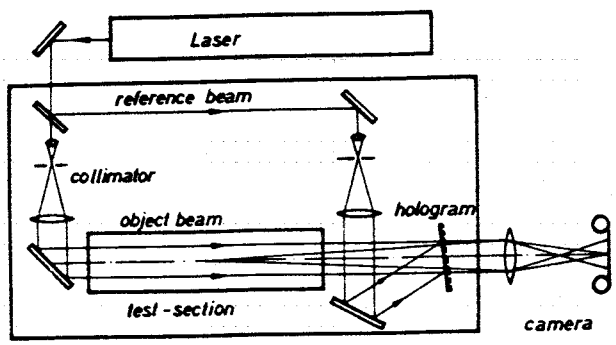

FIGURE 7. Optical set-up for holographic interferometry.

There are many possibilities for arranging the optical set-ups to form a holographic interferometer which cannot be discussed here in detail. Reference is, therefore, made to the literature, for example /7,8/.

Several procedures exist to produce interferograms; here only a sophisticated one which can be used for high-speed cinematigraphy too will be explained. It is called "real-time-method", because it allows to observe a process to be investigated continuously. It is illustrated in FIG.8. After the first exposure, by which the comparison wave is recorded and during which there is no heat transfer in the test section - maybe even no two-phase flow - the hologram is developed and fixed. Remaining at its place or repositioned accurately the comparison wave is reconstructed continuously by illuminating the hologram with the reference wave. This reconstructed wave can now be superposed onto the momentary object wave. If the object wave is not changed and the hologram precisely repositioned no interference fringes will be seen at first (infinite-fringe-field adjustment).

Now the heat transfer process which is to be examined, and for two-phase flow the boiling with bubble formation, or the condensation can be started. Due to this heat transport process a temperature field is formed in the fluid and the object wave receives an additional phase shift passing through this temperature field. Behind the hologram both waves interfere with each other and the changes of the interference pattern can be continuously observed or photographed on still or moving film.

The real-time-method demands an accurate reconstruction of the comparison wave; therefore, the hologram must be repositioned precisely at its original place. This can be done by using a well adjustable plate-holder which, nowadays, can be purchased from the market. It is recommended to use a plate-holder where the final adjustment can be done via a remote control, for example with quartz cristals. The adjustment of the repositioned holographic plate gets its feed-back control signals on an optical basis because the adjustment has to be done in such a way, that the interference fringes - at first visible due to a non-precise position of the plate - disappear during this procedure. This, certianly, has to be done without the heat transfer process having started, however, with the pressure and the temperature under which the system is operated during the experiments.

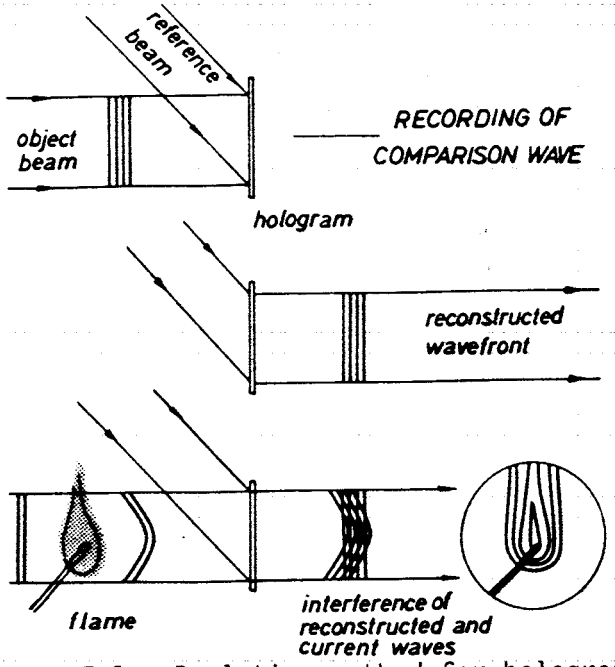

FIGURE 8. Real-time method for holographic interferometry.

If no precisely adjustible plate-holder is available, another procedure can be used. In this case the hologram is not removed after the first exposure by which the comparison wave is recorded but processed at its place. This is done by using a "liquid

plate-holder" consisting of a cuvette in which the photographic plate is inserted. In order to avoid the long drying process and to compensate a shrinkage of the photographic emulsion the plate is soaked in water and also exposed in the cuvette filled with water. Subsequently it is developed and fixed at its place. For the reconstruction the cuvette is filled with water again.

A series of holographic interferograms taken with this method is illustrated in FIG.9, where the bubble formation at a heated surface in water with slow horizontal flow was studied. The water was slightly subcooled, i.e. the bulk temperature of the water was below the saturation temperature, and therefore, the bubble is condensing again after detaching from the heated surface and departing from the superheated boundary layer there.

Another example of the temperature field around a bubble produced and growing on a heated wire shows FIG.10. The interference fringes can be seen more precisely there, and the hologram mediates the interesting information that there is a considerable temperature gradient in the liquid surrounding the bubble near its lower part, where it originated from the wire. This is demonstrated by the interference fringes which we can regard as isotherms in a first, very rough approximation. We have now to discuss how we have to evaluate these interference fringes to get precise information on the temperature field.

In a first step of this evaluation let us assume that there is only a two-dimensional temperature field - not a three-dimensional one like in the

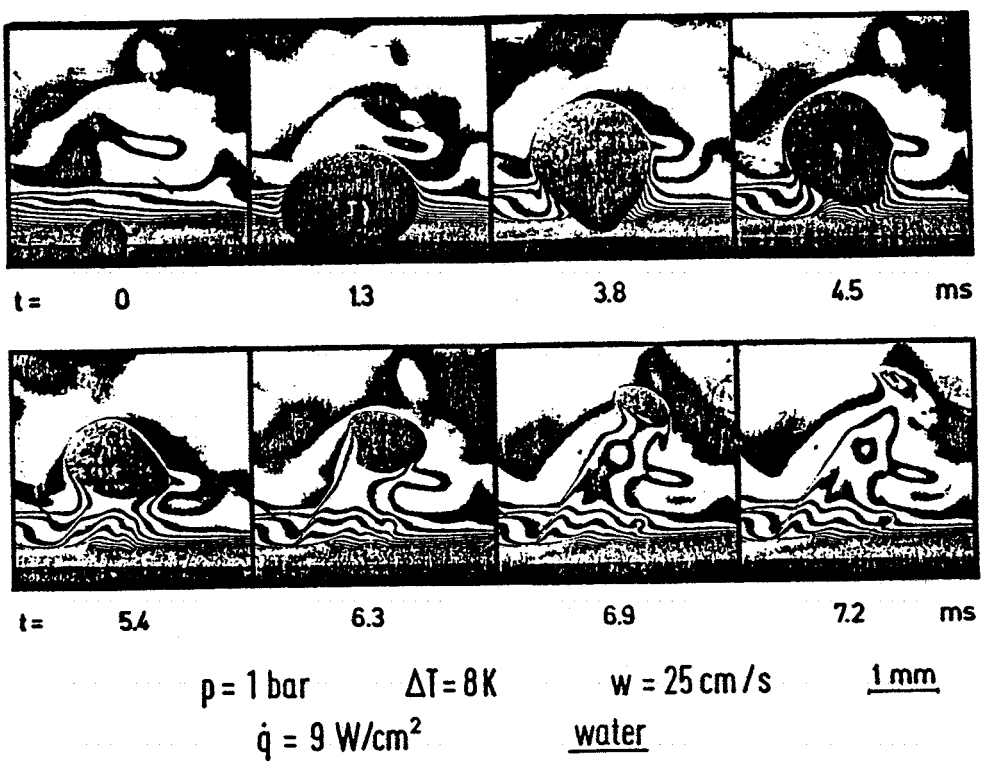

FIGURE 9. Interferogram of boiling water at a heated wall (1 bar, 0,25 cm/s, 8 K subcooling).

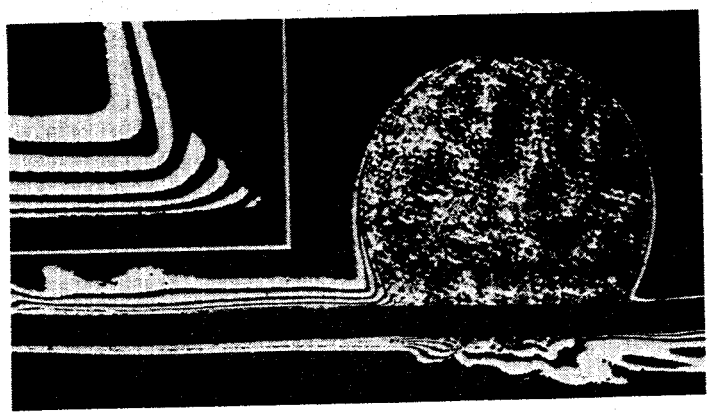

FIGURE 10. Temperature field around a bubble growing at a heated wire.

examples of FIGS.9. and 10. The evaluation of a holographic interferogram made in an optical set-up with parallel object waves is then very similar to the evaluation of interference patterns recorded in a Mach-Zehnder-interferometer /9/. Therefore, here only the basic equations will be given. In Mach-Zehnder-interferometry the wave front, which is distorted by the phase object in the test section, is compared to a plane wave. In holography the object waves passing through the test section at different times are superposed and, therefore, reveal the changes in optical path lengths between the two exposures. Expressed in multiples S of a wave length this change is calculated to

$$S(x,y)\cdot\lambda = l\cdot[n(x,y)_2 - n(x,y)_1] \qquad (1)$$

where l is the length of the test section in which the refractive index n is varied because of temperature changes. The refractive index distribution n(x,y) during the recording of the two waves is - as mentioned above - assumed to be two-dimensional (no variation in light direction). Equation (1) shows that initially only local variations can be determined. Only if the distribution of the refractive index $n(x,y)_1$ during the recording of the comparison wave is known, absolute values can be obtained. Therefore, one usually establishes a constant refractive index field (constant temperature) while recording the temperature wave.

$$S(x,y)\cdot\lambda = l\cdot[n(x,y)_2 - n_\infty] \qquad (2)$$

To abtain absolute values for the temperature field, the temperature at one point in the fluid has to be determined by thermocouple measurements. This is usually done in the undisturbed region or at the wall of the test chamber. Equ.(2) is the equation of ideal interferometry. It is assumed that the light beam propagates in a straight line. Passing through a boundary layer the light beams, however, are deflected because of refractive index gradients. This deflection is used for the various Schlieren- and shadowgraph-methods.

The light deflection can be converted into an additional phase shift ΔS, if a linear distribution of the refractive index is assumed to be within this small area.

$$\Delta S = \frac{n_0 \cdot \lambda \cdot l}{12 \cdot b^2} \tag{3}$$

In this equation b is the fringe width and n_0 is the average refractive index.

In many applications an ideal, two-dimensional field cannot be found. Often the boundary layer extends over the ends of the heated wall, or there are entrance effects or temperature variations along the path of the light beam (axial flow in the test section). Therefore, only integrate values are obtained. Having corrected the interferogram, the obtained refractive index field can be converted into a density field. The relation is given by the Lorentz-Lorenz-formula where N is the molar refractivity and M the molecular mass.

$$\frac{n^2-1}{n^2+2} \cdot \frac{1}{\rho} = \frac{N}{M} \tag{4}$$

If there is only one component in the test section and the pressure is kept constant, the density variations can only be caused by temperature changes. If the fluid is a gas, the situation is very simple because its refractive index is very near to 1, which reduces Equ.(4) to the Gladstone-Dale-equation:

$$\frac{3}{2}(n-1) \cdot \frac{1}{\rho} = \frac{N}{M} \tag{5}$$

With the simple Boyle-Mariotte-law and R as the gas constant we then obtain the following formula, which relates the fringe shift to the temperature:

$$T(x,y) = \left[\frac{S(x,y) \cdot 2 \cdot \lambda \cdot R}{3Npl} + \frac{1}{T_\infty}\right]^{-1} \tag{6}$$

For liquids the procedure is a little more complicated because we have to take in account the real behaviour of the thermodynamic properties as a function of temperature. Therefore, we have to use an equation of state for the refractive index n or we have to take the refractive index from tables interpolating the data with simple equations. Fortunately, there are good data banks avialable in the literature for most of the fluids. However, it is also not difficult to measure the refractive index in a simple optical set-up.

With an equation for the refractive index as function of the temperature we then can use Equ.(1) and we get the connection between the pattern of the interference fringes and the temperature field, as shown in Equ.(7):

$$S(x,y) \cdot \lambda = l \cdot \frac{dn}{dT}\left[T(x,y) - T_0\right] \tag{7}$$

Often local heat transfer coefficients are of special interest. In this case the temperature gradient at the wall is determined and assuming a laminar boundary layer next to the wall or to the phase interface the heat transfer coefficient is obtained by

$$\alpha = \frac{-k \cdot \left(\frac{dT}{dy}\right)_w}{T_w - T_\infty} \tag{8}$$

The assumption that the temperature field is two-dimensional and constant along the path of the beam travelling through the fluid is not valid in case of temperature fields around bubbles. The refractive index n is then a function of the radius r, as demonstrated in FIG.11, and we have to use Equ.(1) in its differential form

$$S \cdot \lambda = \int_0^l (n - n_0) dz \tag{9}$$

and we write it in spherical or cylindrical coordinates:

$$S_{(y)} \cdot \lambda = \int_0^z [n(r) - n_0] \, dz \tag{10}$$

For spherical and cylindrical symmetry Equ.(10) can be solved and integrated as described, for example, by Hauff and Grigull /9/ after transforming it in the form

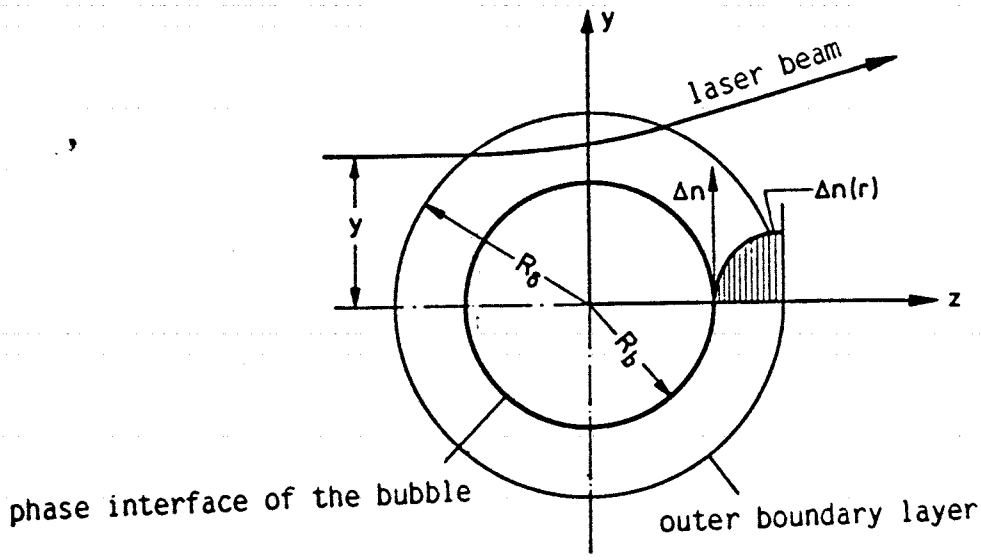

FIGURE 11. Beam deflection and optical conditions in a temperature field around a spherical bubble.

$$S(y)\cdot\lambda = 2\sum_{k=i}^{N-1}\Delta n_K\left[\left(r_{K+1}^2 - r_i^2\right)^{1/2} - \left(r_K^2 - r_i^2\right)^{1/2}\right] \qquad (11)$$

In temperature fields with very high gradients the deflection of the laser beam, which is demonstrated in FIG.11 too, cannot be neglected, as it is done in the evaluating procedure described in /9/. High temperature gradients are especially found in the liquid boundary layer around vapour bubbles, in particular if condensation occurs. In such a case a complicated correction procedure for this deflection has to be used which is described by Nordmann /10/ and by Chen /11/. With the equations and corrections described there, even temperature fields around very tiny bubbles can be evaluated.

Boundary layers at the phase interface are usually very thin - in the order of a few hundredth of a millimeter - and it is difficult to investigate them with the interferometric procedure described up to now, because only a few interference fringes could be observed within this narrow area. Therefore, here another interference method has to be used, the so-called "finite fringe method". In this method, after the reference hologram was produced, a pattern of parallel interference fringes is created by tilting the mirror in the reference beam of FIG.12, or by moving the hologram there within a few lengths. the direction of the pattern can be selected as one likes, and it is only depending on the direction of the movement of the mirror or the holographic plate. This pattern of parallel interference fringes is then destorted by the temperatur field due to the heat transfer process. The distortion or deflection of the fringe from its original - parallel - direction is, in a first rough approximation, the temperature gradient and gives by using Equ.(8) the heat transfer coefficient. A short description how these interference patterns are evaluated, is given in

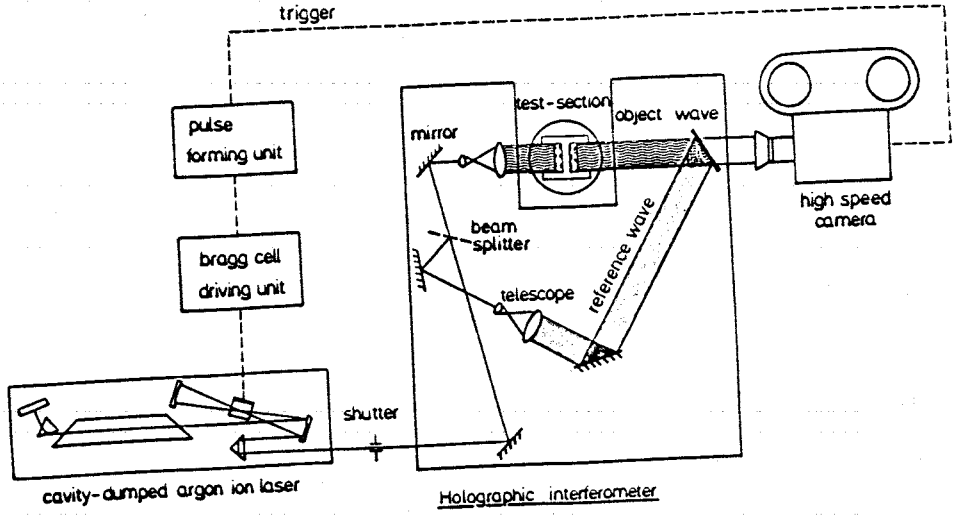

FIGURE 12. Arrangement for holographic interferometry with finite fringe method.

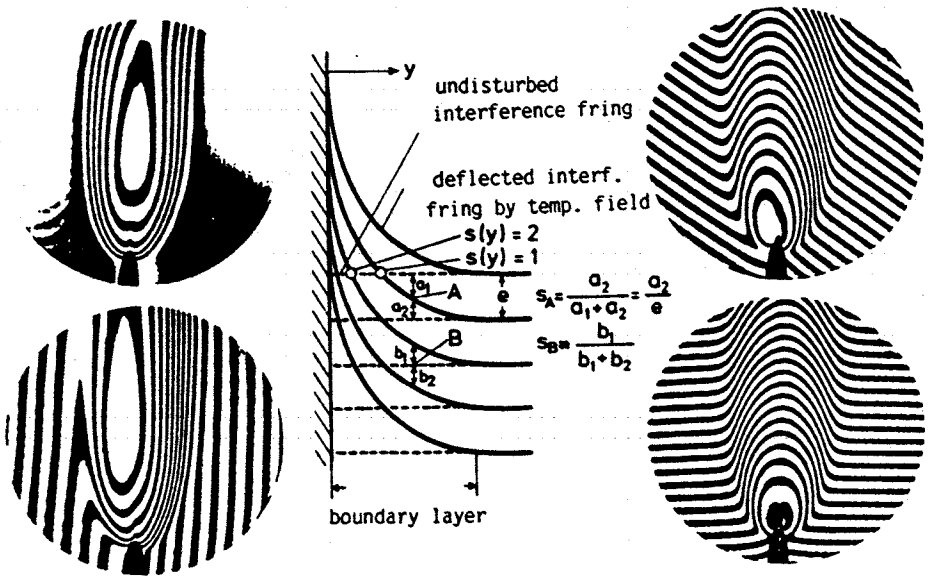

FIGURE 13. Finite fringe interferograms (temperature field around a flame) and their evauation.

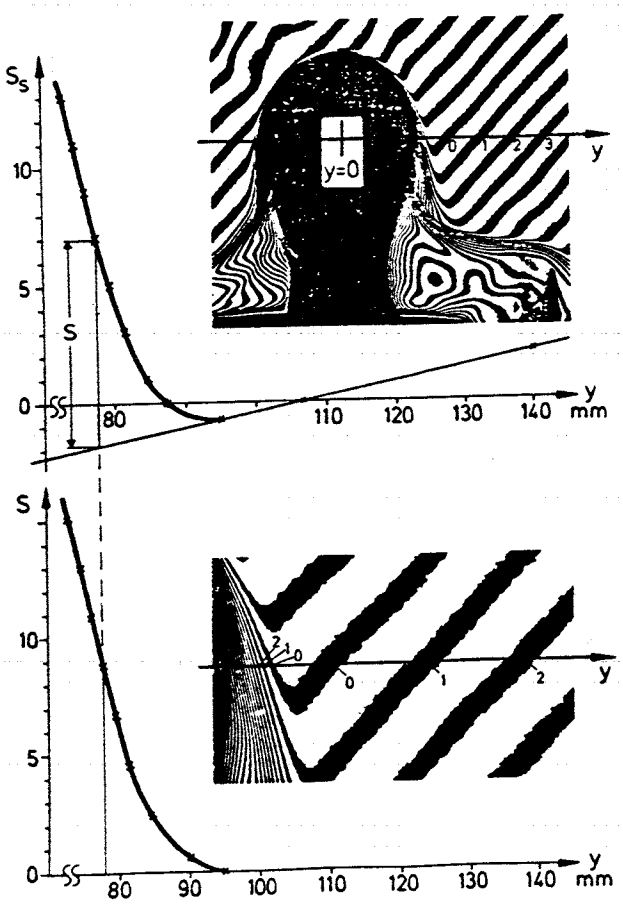

FIG.13. This figure also demonstrates for the example of a temperature field around a burning flame, how these distorted interference fringes look like, depending on the original orientation of the parallel pattern.

FIG.14 and 15 demonstrate the possibilities of using these techniques in flow with bubbles condensing in liquid. FIG.14 illustrates how the temperature field can be evaluated, and FIG.15 demonstrates that this method can be used in high-speed cinematography and allows an inertialess and precise evaluation of the heat transfer coefficient at the phase interface of a condensing bubble.

Holographic interferometry certainly can only be used if the flow situaiton is not too complicated and if the bubble population is not too

FIGURE 14. Interferograms around a condensing bubble and their evaluation.

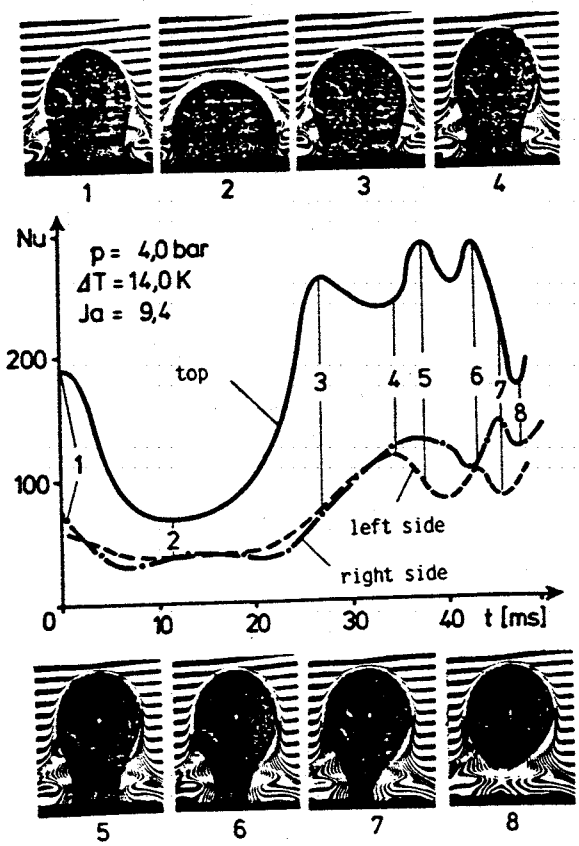

numerous, so that individual bubbles can be identified. It is not possible to look inside the bubbles because the light at the phase interface is totaly reflected. Therefore, the application of this method is limited, as it is the case with all measuring techniques with large temperature gradients in the fluid. Short paths of the light beam have to be verified by a proper arrangement to avoid that too many interference fringes are produced, which could not be evaluated.

FIGURE 15. High-speed cinematography of interferograms around a condensing bubble and the evaluated heat transfer at the phase interface.

Particle size reconstruction from holograms. As mentioned before, in contrast to a photograph, a hologram records an image of three-dimensional scenes which can be reconstructed in their entirety, offering two special advantages especially for investigating swarms of droplets or of particles. When recording the images af entrained droplets, for example, there is no restriction with respect to the depth of field and, furthermore, the reconstructed hologram can be projected in a way in which the magnification of the droplets in the selected focussed plane is uniform.

In order to ensure that particles or droplets are seen as stationary objects, even if they move very fast, a very short exposure time is needed. Therefore, a pulsed laser - usually a ruby-laser - is used, having an exposure time of about 20 ns. An optical set-up to produce holograms with a pulsed laser is shown in FIG.16. A small continuous-wave gas-laser is needed for triggering the pulse of the ruby-laser in case of non-steady flow behaviour. The arrangement of the optical components - like mirrors, wave-expanding lens or holographic plate - is similar to that discussed in the previous chapter.

The reconstructed hologram can be examined by taking photographs of narrow planes of the hologram. Then arises, however, the problem, which particles are exactly in the reconstructed plane and which are protrayed from the volumes just behind or before this selected plane. Therefore, one has to perform a very careful evaluation procedure, defining the sharpness of the

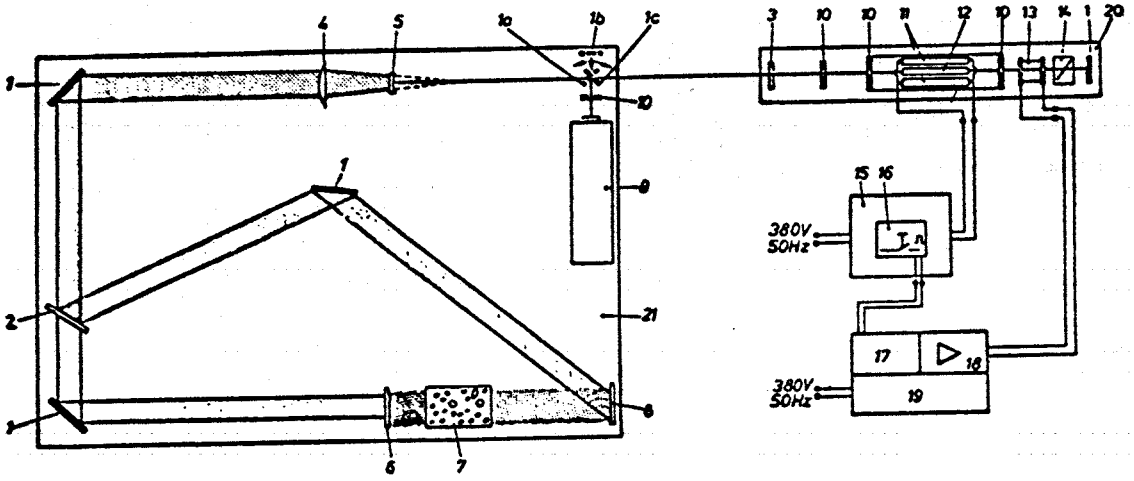

1	mirror, high reflective power	6	diffuser	14	polarization prism
1a	in position for puls-laser adjustment	7	object	15	power supply for flashlights
1b	in position for hologram-recording	8	hologram	16	impulse switch
1c	in position for hologram-reproduction	9	continuous-wave gas laser	17	retarder
2	mirror, semitransparent	10	pinhole	18	power amplifier
3	transparent front mirror	11	flashlight	19	power supply
4	convex lens (f=500 mm)	12	ruby rod	20	laser base-plate
5	concave lens (f=10mm)	13	Pockels cell	21	holography base-plate

FIGURE 16. Holographic set-up with pulsed laser for droplet measurements.

outline of each particle. This procedure shall be briefly described by the example of a droplet swarm - shown in FIG.17 - which is a photograph of a hologram. For further information, reference is made to /12,13/.

The image is digitized by a scanner into discrete pixels with 256 different grey levels with a resolution from 12,5 μm up to 100 μm. A usual 24x36 mm film-format yields to about 345000 points or elements at a resolution of 50 m which have to be processed by a computer code. The processing method is basing on a model for contour-detecting by Robinson /14/, for digitized grey-level images on the basis of differential operations. A detailed description of the method is to be found in /12/.

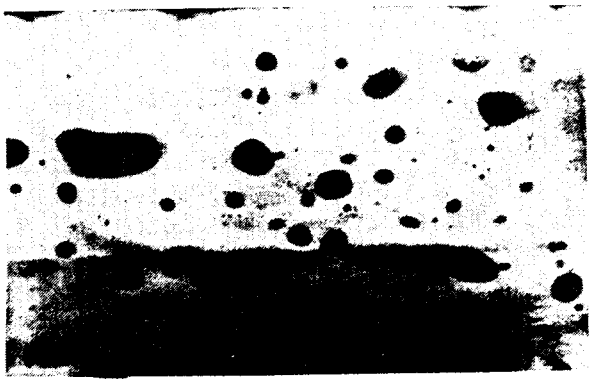

FIGURE 17. Hologram of a droplet swarm.

In a first step the outlines of the particles are detected by a gradient calculation for each pixel, checking whether its grey value is lower than a given level and comparing the pixel with 8 adjacent pixels. Then, by means of a differential operation, the direction and the value of the grey gradient are determined in this point. Additionally, further examinations are performed by comparing the gradient direction for each pixel with the pixels surrounding it, and then the pixel is separated by using a defined gradient level operator. So by producing grey level gradients, one can distinguish between a sharp, a slightly indistinct and a blurred droplet. Then the photograph of the hologram can be reconstructed by the computer and - for a better distinction - the droplets with sharp outlines being exactly in the focussed plane of the reconstructed image are hatched, as shown in FIG.18. Now the circumference and the cross-section area of the selected drops can be determined and, from this, one finds with the usual methods mean droplet diameters, like the Sauter-diameter or the droplet size distribution.

2.2 Non-image Forming Methods.

Non-image forming methods can give averaged values as well as local ones. As "sensors" these methods can use visible or non-visible light and other waves, like electro-magnetic ones or ionizing rays like γ-, β-, or X-rays. Also the use of sound waves as sensors in two-phase flow is proposed in the literature.

Most of these methods were especially developed for investigations in spray- or fog-flow. The benefit of these methods is that - contrary to the image-forming procedure - they give also certain information, if the mean droplet diameter is below 10 μm. The methods can be used for measuring the droplet size and the droplet concentration as well as for determining the droplet velocity.

Droplet measurements by light scattering and light diffraction. There are numerous proposals in the literature for methods to measure the size and concentration of droplets or aerosols in flowing vapour or gas. Here only a very brief description of the principles of these methods can be given. For more detailed information reference is made to /15-19/. The possibilities of applying this modern instrumentation for industrial particle measurements are described in /20/.

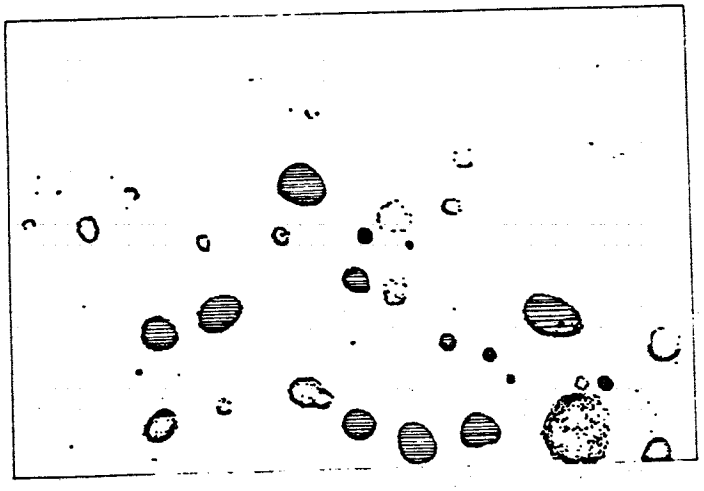

FIGURE 18. Reconstruction of a focussed plane of a hologram.

Scattering is an indirect method of fine particle characterization. The size of the particle is inferred from the properties of scattered light, using a calibration curve or a theoretical analysis. For calibrating a swarm of

droplets or particles has to be produced with well-known diameter and density.

In scattering instruments an aerosol or a tiny droplet is illuminated by an expanded laser beam and the light diffracted by each particle is imaged onto a photovoltaic detector by a lense positioned on the axis of the laser. The diffraction patterns from each particle are superimposed on this plane, so the angular width of the diffraction lobe is determined by the size distribution of the particles or droplets in the beam. If the particle diameters are very much greater than the wave lengths of the illuminating light, the scattering properties can be predicted using the "Fraunhofer diffraction theory". This theory says that for small angles around the direction of the incident ray and for particle sizes much greater than the light wave length the intensity of the diffracted light is independent of the optical characteristics of the particles and depends only upon their size.

The diffracted intensity versus the observation angle shows a sequence of maxima and minima which on a screen generated a series of alternatively bright and dark concentric annuli whose diameters change with the size of the particle. The "Malvern particle size analyser", proposed by Swithenbank /21/, is based on this principle. Its optical arrangement is shown in FIG.19. Photodiode detector rings are placed in the focal plane of the lens. The receiving areas increase by three orders of magnitude from the center to the periphery in order to compensate for the reduction of the diffracted light. In its normal mode of operation this instrument gives the cumulative size distribution by particle weight in a spatial average of all particles in the beam. Brown and Felton /22/ proposed methods for using this instrument in measuring both, size distributions and concentrations of non-spherical particles.

Another instrument using light scattering techniques for droplet- and particle-Measurements is the "single particle counter". This instrument produces a region of intense illumination, usually at the focus of a laser which is called the "probe volume". When a particle passes through the probe volume, the light scattered is collected by a lens which is focussed onto the probe volume. The collected light is transmitted to a photovoltaic detector, from where the signal is electrically processed.

Finally, the polarization method has to be mentioned. This method uses the polarization ratio which is defined as the ratio of the light fluxes measured in the planes perpendicular and parallel to the direction of the illuminating beam and the direction of observation /23/. This ratio is independend of the particle number density in the test volume, if monodispersed particles are present and if no multiple diffusion occurs. So

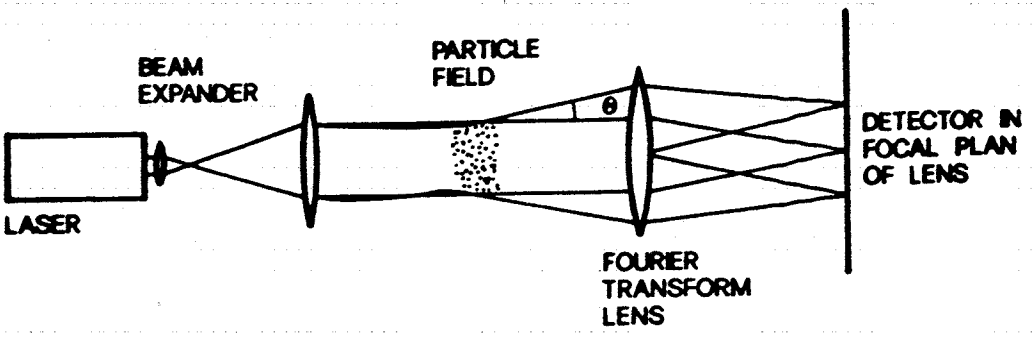

FIGURE 19. Optical arrangement of the Malvern particle size analyzer.

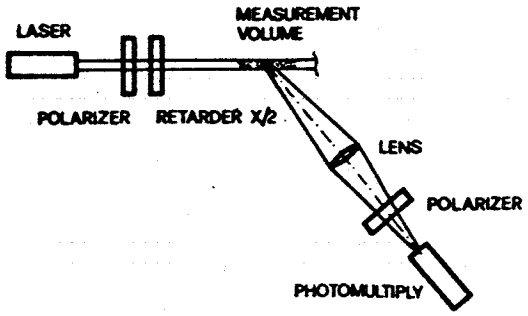

the polarization ratio is a function of the particle diameter. The principal optical arrangement of this method is shown in FIG.20. The dependency of the polarization ratio on the particle diameter can be calculated by using Mie's theory.

FIGURE 20. Optical arrangement of the polarization method for measuring particle diameters.

In the case of polydispersed particles the values of the polarization ratio depend on the granulometric distribution of the particles in the test volume. Here - to a certain extent - a calibration or the assumption of a distribution function is necessary to evaluate the data.

Finally, one can also use the absolute intensity of the light behind the droplet swarm to measure droplet sizes. Here Mie's theory is used, too, to get the relationship between the diffused light intensity and the sizes of droplets, if their optical characteristics are known. The diffused intensity is a monotonous function of the diameter of the droplets. From a certain value of droplet diameters on this intensity shows a non-monotonous behaviour.

Laser-Doppler methods. The Laser-Doppler-anemometry originally was a method for measuring the local velocity in single-phase flows. The basic phenomenon used by this method is the frequency-shifting of light scattered by particles which have a relative motion to the light direction. A simple arrangement with a reference beam is shown in FIG.21. The incoming laser beam is split into two beams, the reference beam and the scattering beam. After passing a focussing lens the reference beam is reduced by an intensity filter before it reaches the measuring volume. Both, the reference beam and the light scattering from the moving particles in the small volume under investigation, are received by a photomultiplier. The difference in frequency between the two beams is proportional to the velocity of the particles.

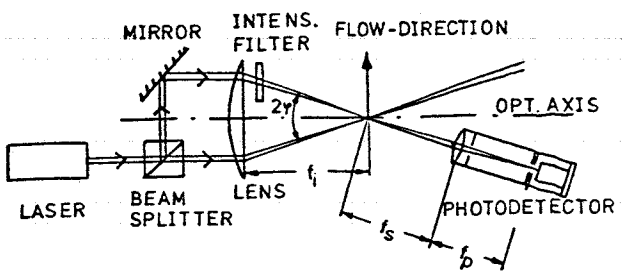

Durst and his co-workers /24-26/, as well as Saffman /27/, developed this method for the use in dispersed flow systems and extended it to droplet- or bubble-diameters in order of some millimeters. In this range of droplet size the Doppler shift-frequencies have to

FIGURE 21. Simple Laser-Doppler anemometer.

be calculated by using geometrical optics. The paper by Durst and Zaré /26/ describes the instrumentation to measure particle size and velocity in two-phase flow and gives a detailed description of the fringes formed in space by the interference between the reflected, refracted and diffracted light from the droplet or particle surface when it passes through the measuring volume. There are 12 possible interference fringe patterns which can be produced by the two beams passing into and out of an arbitrary shaped particle. Durst and Zaré showed that the rate at which fringes cross the detector is linearly related to the velocity of the reflecting surface, perpendicular to the axis of the beams. This allows velocity measurements in two-phase flow. For perfectly reflecting spheres the back-scattered fringes are plane-parallel and their separation Δx follows the equation

$$\Delta x = \left[1 + \frac{2(L-r)}{2\cos\alpha}\right] \frac{\lambda}{2\tan\alpha} \qquad (12)$$

In this equation is
L = the distance between the probe volume and the detector,
r = the radius of the sphere,
α = the crossing angle of the beams, and
λ = the wave length.

The radius of the sphere can be obtained by measuring the fringe distance Δr in the backward direction. for the case of a transparent sphere the fringe spacing in the region of the optical axis is given by

$$\Delta x = \left[1+2\left(\frac{n_1}{n_2}-1\right)\frac{L}{r}\right] \cdot \frac{\lambda}{2n_1\alpha} \qquad (13)$$

where n is the refractive index outside of the sphere and n_2 inside of it. Both equations are only valid for small beam crossing angles and large ratios L/r. Durst and Zaré suggest that with knowing the relationship between the fringe spacing and the observation distance one can determine also changes in the shape and in the size of the droplets or bubbles by using the phase difference between the signals, if several Doppler-detectors are available which are viewing the measured volume from different angles. The use of this special Doppler method and the Laser-Doppler anemometer signals are an important alternative to the visibility techniques for measuring size-changings of bubbles and droplets.

Raman scattering method. Raman scattering is well recognized as a powerful tool for investigating molecular structures. In the early 1960's the method found application to fluiddynamic studies and also to temperature measurements in single-phase flow. Recently there came up studies /28/ using this method for temperature measurements in non-equilibrium dispersed two-phase flow, too.

In a two-phase water sample, for example, there is potential for spectral interference between Raman bands for the liquid- and vapour-phases. The 3400 cm^{-1} band for liquid water is broader than the 3650 cm^{-1} band for water vapour, due to molecular interactions such as hydrogen bonding.

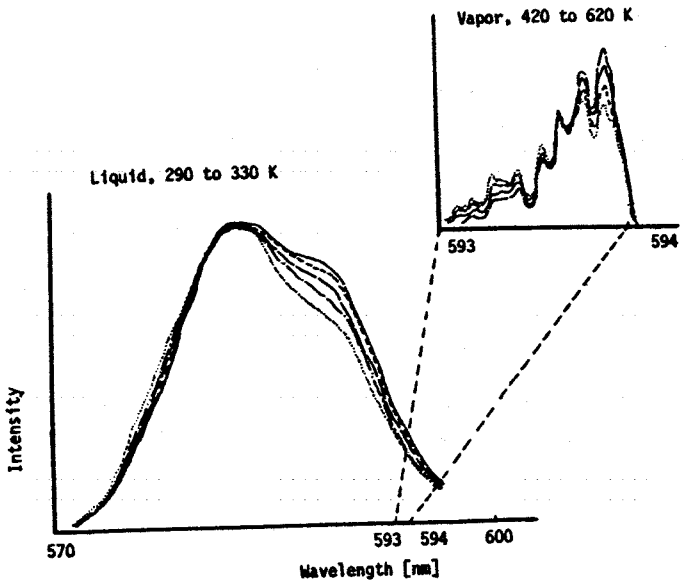

FIG.22 shows the Raman vibrational bands for both, the liquid and vapour phases. The liquid band overlaps the spectral region of interest for the vapour. For relatively high void fractions Raman scattering from the liquid phase is expected to cause minimal interference.

FIG.23 shows a Raman system used in non-equilibrium dispersed flow samples of water-vapour-mixtures /28/. The laser irradiates the sample with an intense beam of high-

FIGURE 22. Raman scattering from water and steam.

frequency monochromatic light. The incident beam is concentrated on the measurement point by the focussing optics. The path of the incident beam through the sample defines the scattering volume. The collection optics focus scattered light onto the entrance slit of the premonochromator. The premonochromator filters the scattered light transmitting a selected spectral band to the spectograph. The spectograph, driven by a microprocessor-controlled stepping motor, sweeps the selected spectral band. The photomultiplier tube optimized for photon-counting detects the spectral intensity distribution. The photomultiplier output is amplified and recorded by a multi-channel analyzer.

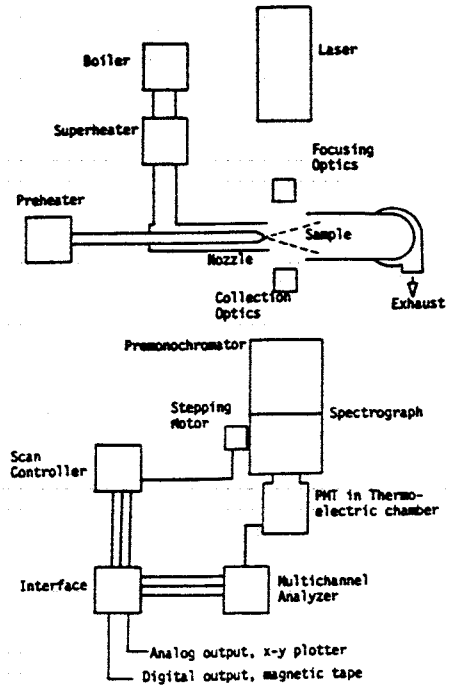

FIGURE 23. Arrangement for vapour-temperature measurements in two-phase flow.

3. NON-OPTICAL METHODS

Instead of optical waves also ionizing rays, like γ-, β- or X-rays, can be used as sensors in two-phase mixtures. In the literature also electro-magnetic waves and even sound waves are proposed for measuring distribution and density of the dispersed phase and also the velocity of the phases. These methods are either using the attenuation of the rays, with and without image-forming, or the Doppler-effect of scattered or reflected waves.

3.1 γ-Ray Attenuation Techniques

The γ-ray technique is based on a high energy radiation - in this case -radiation - which, while penetrating substance, is attenuated. The degree of attenuation is depending on the density of the substance through which the ray travels. This means for gas-liquid-mixtures that the attenuation is high if only liquid is in the volume under investigation, and decreases with increasing gas content or void. It has, however, to be taken in account that the radiation is also attenuated in the structure material, for example the wall of the tibe containing the two-phase flow or the flow channel.

Usually Cesium 137 or Iridium 192 is used as a source for the γ-ray. Cesium has the advantage of a long decay time which means that the source can be used for a long time without re-calibratung the intensity of it. Iridium is emitting more softer rays and, therefore, offers a better solution of its signals in gas-liquid-mixtures compared to Cesium, however, it has the drawback of a short decay period.

The spheric waves originating from the γ-source first hit - as demonstrated in FIG.24 - a plate of lead in which a narrow slot or a small hole is placed. This forms a thin, well-bundled -ray which penetrates the two-phase flow channel. That lead plate is called collimator. Behind the flow channel another collimator is placed. Both collimators prevent that scattered γ-rays - due to primary or secondary effects - hit or enter into the detector and, by this, falsify the reading. The detector registering the γ-quants may be a Geiger-counter in a simple case, or a sodium-jodite-crystal which produces flashes of light proportional to the number of incoming γ-quants. These flashes of light are transformed in electrical signals via a phototransistor and then evaluated electronically. The intensity I of the emitted ray measured in photons per cross section of the ray and time is proportional to the intensity I_o of the ray entering the two-phase flow channel and

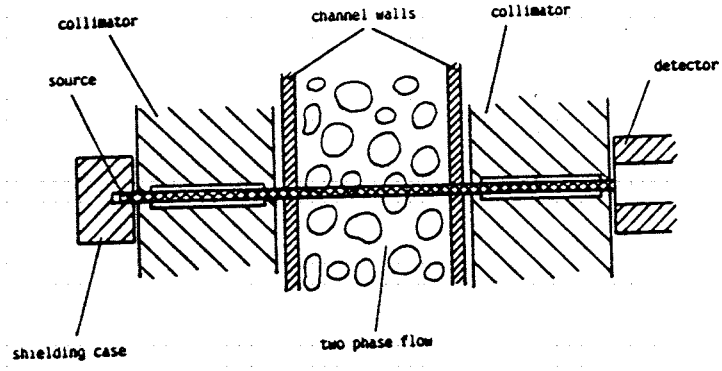

FIGURE 24. Prinziple arrangement of the γ-ray attenuation method.

an exponential function of the densities of the penetrated substances and the length l of the path the ray is travelling /29/.

$$I = I_o \exp\left[-(\mu_W \rho_W \cdot l_W + \mu_L \rho_L \cdot l_L + \mu_V \rho_V \cdot l_V\right] \qquad (14)$$

In Equ.(14) μ is a substance-specific absorption coefficient which, however, with a single component gas-liquid flow has the same value for the liquid- and for the vapour-phase. The exact knowledge of the absorption coefficient and of the travelling length l of the γ-ray through the structure material - for example the wall - is not necessary if a calibration is used during which only two measurements have to be performed. One measurement has to be done with the channel filled with liquid, giving the intensity I_2, and the second one with only vapour or gas in the channel, from which one reads the intensity I_1 at the detector. The local volumetric void ε existing during the experiment in the channel results then from the momentary intensity I registered by the detector.

$$\varepsilon = \frac{\ln(I/I_2)}{\ln(I_1/I_2)} \qquad (15)$$

From Equ.(15) it can be easily seen that the accuracy of this measuring technique is low with high voidage and also in the vicinity of the critical state of the fluid, i.e. if the densities of vapour and liquid are in the same order of magnitude. At high void fractions the intensity I of the γ-ray is almost the same as that in pure vapour flow. The accuracy of this measuring technique is also depending on the statistical fluctuations resulting from the decay of the γ-source, and also resulting from the imission of the atmosphere. The latter one can be produced by shielding or by a special compensating arrangement of two detectors, where the second one is only measuring the imission from the atmosphere.

For getting informations over the whole cross section of the flow channel or on an averaged value in the channel one has to move the whole arrangement, as shown in FIG.22, perpendicular to the flow direction. Special care has to be taken that during this movement the collimators and the detector are always made exactly straight along one line because small deviations in the alignment may cause serious misreadings.

The moving of the γ-ray perpendicular to the flow channel takes much time and is, therefore, not suitable for fast changing transients in the flow. In the literature, therefore, several arrangements are proposed using more than one γ-ray penetrating the channel at the same time in different directions. One example of such an arrangement is shown in FIG.25. Two γ-sources placed immediately in front of the flow channel during the measuring period are emitting γ-rays. These rays after penetrating the flow channel can enter five paths drilled into a block of lead at which ends five detectors are placed. So one gets a reading of each of the five penetration angles through the flow channel. A special method has then to be used, for example the tomography, to evaluate these readings for reconstructing the two-dimensional distribution of the void fraction in the flow channel which gives information on the flow pattern too. For transient measurements γ-sources of high power - 5 to 10 Curie - are needed to allow short periods - a few milliseconds - for signal recording.

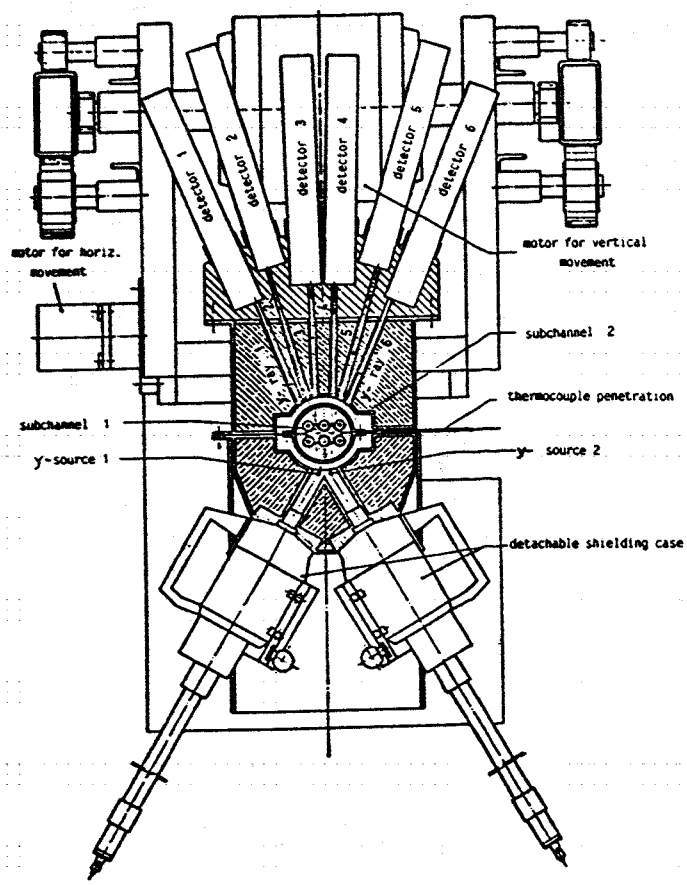

FIGURE 25. Multiple beam arrangment for γ-ray attenuation technique.

3.2 X-ray Image Forming Techniques

Instead of the γ-ray also an X-ray can be used. X-rays have the advantage that instruments are commercially available which allow to record the attenuation in a large area and form an image of the penetrated volume. This X-ray technique is well-known in daily life, as for example in medicine, in material testing or nowadays also for checking the luggage of airplane passengers.

The radiation source in this case is an X-ray tube which can produce extremely short flashes by using a special electronic device and, by this, also highly transient processes can be investigated. An example for an arrangement of such an X-ray apparatus is shown in FIG.26. The evaluation of the picture produced by this arrangement is made by an image transformer which makes visible the different intensities, due to attenuation of the X-ray in form of darker of lighter grey tones on a photographic plate or even on the film of a movie camera.

With the help of a television camera these grey tones can again be transformed in different colours, giving a stepwise information of the X-ray attenuation in the channel and, by this, of the void fraction and its distribution in the flow.

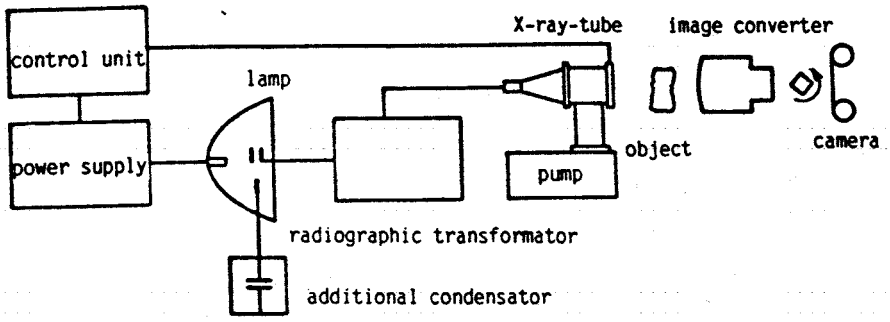

IGURE 26. Example of an X-ray flashing unit.

.3 Sound Waves

here are also several proposals to use sound waves for detecting bubbles in iquid flow and even for determining their travelling velocity. Korte and übbert /30,31/ recently reported a method for measuring the bubble velocity ven in muddy fluids, for example broths in biotechnical processes based on ltrasonic-Doppler-pulse technique. Only one ultrasonic device is needed which lternatively is used as emitter or as receiver. The wave is reflected at the pposing wall.

he energy of the ultrasonic waves registered by the detector is depending on wo competing effects. On the one side this energy is proportional to the pro- uct of the number of bubbles in the flow and the effective cross section area f the reflectors in the scattering volume. This product is proportional to the pecific phase interface. On the other side the transmission of the ultrasonic aves is reduced exponentially with increasing specific phase interface. The ntensity of the ultrasonic wave registered at the detector, therefore, is a unction of the specific phase interface. This relationship can be taken as a alibration help for calculating the specific phase interface from the measured ignal energy.

EFERENCES

1. Arnold, C. R., Hewitt, G. F., Further Developments in the Photography of Two-Phase Gas-Liquid Flow, Journal of Photographic Science 15 (1967)97.

2. Langner H., Untersuchungen des Entrainmentverhaltens in stationären und transienten zweiphasigen Gemischen, Diss. Technische Universität Hannover, 1978.

3. Gabor D., A New Microscopic Principle Nature 161, 777 (1948), Microscopy by Reconstructed Wave-fronts, Proc. Roy. Soc. A 197, 454 (1949), Microscopy by Reconstructed Wave-fronts II, Proc. Phys. Soc. B 64, 449 (1951).

4. Smith, H. M., Principles of Holography, Wiley (Interscience), New York (1969).

5. Caulfield, H. J. and Sun Lu, The Applications of Holography, Wiley (Interscience), New York (1970).

6. Collier, R. J., Burckhardt, C. B. and Lin, L.H., Optical Holography, Academic Press, New York (1971).

7. Mayinger, F., Panknin, W., Holography in Heat and Mass Transfer, 5th Int. Heat Transfer Conference, Tokyo, 1974.

8. Panknin, W., Eine holographische Zweiwellenlängen-Interferometrie zur Messung überlagerter Temperatur- und Konzentrationsgrenzschichten, Diss. Technische Universität Hannover, 1977.

9. Hauf, W. and Grigull, U., Optical Methods in Heat Transfer, Advances in Heat Transfer 6, 133, Academic Press Inc., New York 1970.

10. Nordmann, D., Temperatur, Druck und Wärmetransport in der Umgebung kondensierender Blasen, Diss. Universität Hannover, 1980.

11. Chen, Y. M., Wärmeübergang an der Phasengrenze kondensierender Blasen, Diss. Technische Universität München, 1985.

12. Hawighorst, A., Untersuchungen zur Tropfengrößenbestimmung, Diss. Universität Hannover, 1985.

13. Hawighorst, A., Kröning, H., Mayinger, F., Fluid Dynamic Effects in the Fuel Element Top Nozzle Area During Refilling and Reflooding, Nucl. sci. engng. 88 (1984), Nov. S. 376-384.

14. Robinson, G. S., Edge Detection by Compass Gradient Masks, Computer Graphics and Image Processing, Vol. 6, No. 5, 1977.

15. Boron, S. and Waldie, B., Particle Sizing by the Forward Lobe Scattering Technique: Errors Introduced by Applying Diffraction Theory in the Mie Region, Appl. Opt. Vol. 17, No. 10, pp. 1644-1648, 1978.

16. Bachalo, W. D., Method for Measuring the Size and Velocity of Spheres by Dual-Beam Light Scattering Interferometry, Appl. Opt. Vol. 19, No. 3, pp. 363-370, 1980.

17. Negus, C. R. and Drain, L. E., Mie Calculations of the Scattered Light from a Spherical Particle Traversing a Fringe Pattern Produced by Two Intersecting Laser Beams. J. Phys. D (London), Appl. Phys., Vol. 15, pp. 375-402, 1982.

18. Brown, D. J. and Felton, P. G., Direct Measurement of Concentration and Size of Particles of Different Shapes Using Laser Diffraction, Chem. Eng. Res. Des., Vol. 63, pp. 125-132, 1985.

19. Hemsley, D. J. and Yeoman, M. L., Calibration Techniques for a Single Particle Monitoring System Using Forward Diffraction Doppler Signal Visibility, Proc. of 5th Particle Size Analysis Conf., John Wiley and Son, pp. 183-191, 1985.

20. Liu, B. Y. H., Applications of Modern Aerosol Instrumentation for Industrial Particle Measurement, 3rd European Symp. on Particle Characterisation, Partec'84, Nuremburg, Germany, pp. 501-513, 1984.

21. Swithenbank, J., Beer, J. M., Taylor, D. S., Abbot, D. and McGreath, C. G., A Laser Diagnostic Technique for the Measurement of Droplet and Particle Size Distributions, A.I.A.A. Progress in Astronautics and Aeronautics, A.I.A.A.N.Y. (Ed. Zinn, B.T.), Vol. 53, pp. 421-477, 1977.

22. Azzopardi, B. Measurement of Drop Sizes, Int. J. Heat and Mass Trans., Vol. 22, pp. 1245-1279, 1979.

23. D'Alessio, A., Cavaliere, A., Menna, P., Theoretical Models for Interpretation of Light Scattering by Particles Present in Combustion Systems, Soot in Combustion Systems and its Toxic Properties, 1983.

24. Durst, F., Melling, A. and Whitelaw, J. H., Princles and Practice of Laser Doppler Anemometry, Academic Press, Second Edition, 1981.

25. Durst, F. and Umhauer, H., Local Measurement of Particle Velocities Size Distribution and Concentration with a combined Laser Doppler Particle Sizing System, Proc. of the LDA Symp. Copenhagen, pp. 430-456, 1975.

26. Durst, F. and Zarê, M., Doppler Measurements in Two Phase Flows, Proc. of the LDA Symp., Copenhagen, pp. 403-429, 1975.

27. Saffman, M., Buchave, P. and Tanger, H., Simultaneous Measurements of Size, Concentration and Velocity of Spherical Particles by a Laser Doppler Method, Int. Symp. on Appl. LDA to F. Mech., Lisbon 84, Section 8.1, 1984.

28. Anastasia, C. M., Neti, S., Smith, W. R., Chen, Y. M., Raman Scattering Temperature Measurements for Water Vapour in Nonequilibrium Dispersed Two-Phase Flow, NUREG/CR-2905 (U.S. Nuclear Regulatory Commission).

29. Schrock, V. E., Radiation Attenuation Techniques, Two-Phase Flow Instrumentation, 11th National ASME/AICHE Heat Transfer Conference, Minnesota, 1969.

30. Lübbert, A., Korte, Th., Fortschritte beim Ultraschall-Doppler-Verfahren, Chem. Ing. Techn. 59 (1987) Nr. 1, S. 84-85.

31. Korte, Th. , Lübbert, A., Chem. Ing. Techn. 57 (1985), S. 1114-1115, MS 1428/85.